Structural Origins of Redox Potentials in Fe-S Proteins: Electrostatic Potentials of Crystal Structures

Paul D. Swartz,* Brian W. Beck,# and Toshiko Ichiye#
*Center for Bioengineering, University of Washington, Seattle, Washington 98195-1750, and #Department of Biochemistry/Biophysics, Washington State University, Pullman, Washington 99164-4660 USA

ABSTRACT Redox potentials often differ dramatically for homologous proteins that have identical redox centers. For two types of iron-sulfur proteins, the rubredoxins and the high-potential iron-sulfur proteins (HiPIPs), no structural explanations for these differences have been found. We calculated the classical electrostatic potential at the redox site using static crystal structures of four rubredoxins and four HiPIPs to identify important structural determinants of their redox potentials. The contributions from just the backbone and polar side chains are shown to explain major features of the experimental redox potentials. For instance, in the rubredoxins, the presence of Val 44 versus Ala 44 causes a backbone shift that explains a ~50 mV lower redox potential in one of the four rubredoxins. This result is consistent with experimental redox potentials of five additional rubredoxins with known sequence. Also, we attribute the unusually lower redox potentials of two of the HiPIPs studied to a less positive electrostatic environment around their redox sites. Finally, molecular dynamics simulations of solvent around static rubredoxin crystal structures indicate that water alone is a major factor in dampening the contribution of charged side chains, in accord with experiments showing that mutations of surface charges produce relatively little effect on redox potentials.

INTRODUCTION

Elucidation of the structure-function relationships of electron transfer proteins is crucial for understanding electron transport at a molecular level. One important property of an electron transfer protein is its redox potential, which not only affects electron transfer rates but must also be matched to the redox potentials of its electron transport partners. However, proteins with apparently the same redox center can have different redox potentials, which shows that the protein itself influences the redox potential. Understanding how proteins are able to accomplish this is thus critical for understanding biological electron transfer.

Iron-sulfur proteins are an important class of electron transfer proteins because of the wide variety of biological reactions in which they participate and the wide variety of organisms in which they are found (Cammack, 1992; Matsubara and Saeki, 1992; Armstrong, 1982). This work focuses on two types of iron-sulfur proteins that represent two very different cases: the rubredoxins (M_r = 6000) and the high-potential iron-sulfur proteins, or HiPIPs (M_r = 8000). The redox site in rubredoxin, which is located close to the protein surface, consists of an iron tetrahedrally ligated to four cysteinyl sulfurs (the 1Fe site) (Fig. 1 *a*). High-resolution crystal structures have been solved for rubredoxins from five species (Frey et al., 1987; Watenpaugh et al., 1980; Sieker et al., 1986; Adman et al., 1991; Day et al., 1992), four of which have reported redox potentials ranging from −57 to 6 mV (Moura et al., 1979; Lovenberg and Sobel, 1965; Adams, 1992; LeGall et al., 1988). The five rubredoxin structures are all highly similar in backbone structure and have ~50 to 60% sequence identity (Fig. 2 *a*). Despite the similarity, one of these rubredoxins has a redox potential that is ~60 mV less than the three others with reported values. The redox site in the HiPIPs, which is buried deep within the protein, consists of four irons and four inorganic sulfurs arranged in a cubanelike structure with the irons ligated to four cysteinyl sulfurs (the 4Fe-4S site) (Fig. 1 *b*). High-resolution crystal structures for four HiPIPs have been solved (Carter et al., 1974; Breiter et al., 1991; Rayment et al., 1992; Benning et al., 1994), which have redox potentials ranging from 120 to 360 mV (Meyer et al., 1983). The tertiary structures of these HiPIPs adopt similar folds, but their primary sequences have only 11% sequence identity and very little sequence similarity (Fig. 2 *b*), and the loops that extend from the core of the protein vary considerably in size. Interestingly, whereas the two HiPIPs of intermediate size have redox potentials near 130 mV, the smallest and largest HiPIPs both have redox potentials near 350 mV, indicating that the variation in redox potential is not simply a size effect. Thus, the four rubredoxins studied have highly similar sequences and structures with a very small redox site located close to the surface of the protein, whereas the four HiPIPs studied have only limited similarities in sequence and structure with a somewhat larger redox site buried within the protein.

The possible sources for differences in redox potentials for proteins with the same types of Fe-S sites have been reviewed previously (Sweeney and Rabinowitz, 1980). For instance, the protein could distort the redox site, thus changing the intrinsic ionization potential of the site. However, many examples exist where several crystal structures show little variation of the redox-site geometry for proteins with

Received for publication 12 March 1996 and in final form 27 August 1996.
Address reprint requests to Toshiko Ichiye, Department of Biochemistry and Biophysics, Washington State University, Pullman, WA 99164-4660. Tel.: 509-335-7600; Fax: 509-335-9688; E-mail: ichiye@wsu.edu.

0006-3495/96/12/2958/12 $2.00

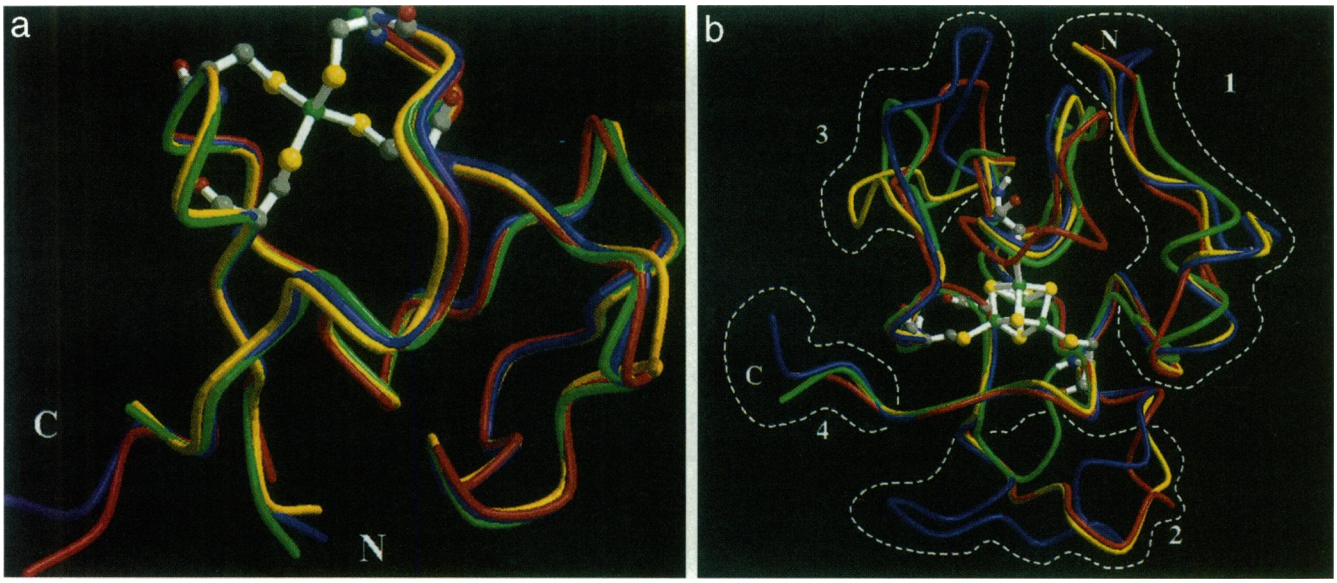

FIGURE 1 Rubredoxin and HiPIP structures. (*a*) Superposition of the backbone of the four rubredoxins *C. pasteurianum* (*blue*), *D. gigas* (*green*), *D. vulgaris* (*yellow*), and *P. furiosus* (*red*) showing the position of the redox site. (*b*) Superposition of the four HiPIPs *C. vinosum* (*blue*), *E. halophila* (*red*), *R. tenuis* (*green*), *E. vacuolata* (*yellow*) showing the position of the redox site and the positions of variable and core domains. Cysteine residues and redox-site atoms are represented in ball-and-stick. Variable domains are set off by dashed white lines. Amino-termini and carboxyl-termini are marked "N" and "C" respectively. These figures were generated using MOLSCRIPT (Kraulis, 1991) and Raster3D (Merritt and Murphy, 1994).

the same Fe-S site. In addition, resonance Raman spectroscopy indicates that the range of redox potentials seen in HiPIPs cannot be ascribed to the differences in redox-site structure (Backes et al., 1991). Moreover, recent electronic structure studies to quantify the degree of geometric deviation necessary to cause a variation in the redox potential support the idea that the observed differences in the redox-site structures are not responsible (Koerner and Ichiye, submitted for publication).

If the redox-site structure does not vary, the differences must lie in the protein itself. However, despite the existence of several high-resolution structures for rubredoxins and HiPIPs, along with experimentally measured redox potentials, to date there are no confirmed structural motifs that can be linked to the redox potential differences for either type of protein. For instance, although the number of hydrogen bonds from backbone amide hydrogens to the cysteinyl sulfurs apparently plays a role in differentiating the redox potentials of the HiPIPs from the ferredoxins (Adman et al., 1975; Backes et al., 1991), resonance Raman spectroscopic and x-ray crystallographic studies suggest that it is not significant in determining differences of homologous iron-sulfur proteins (Breiter et al., 1991; Rayment et al., 1992; Backes et al., 1991). Other studies of HiPIPs indicate that no correlation exists between the location of aromatic residues and the redox potential (Rayment et al., 1992).

Another source of differences in the redox potentials of proteins is the electrostatic potential due to the surrounding protein and solvent (Churg and Warshel, 1986; Gunner and Honig, 1991; Langen et al., 1992b; Shenoy and Ichiye, 1993). Of the various possible types of electrostatic potential contributions in a protein, several results suggest that charged side-chain residues at the surface contribute little to the redox potential (Schejter and Eaton, 1984). For instance, experiments on redox proteins in which an amino acid residue is mutated to or from a charged residue show relatively minimal or otherwise inconsistent effects on the redox potential (Shen et al., 1994; Gleason, 1992; Zeng et al., 1996), possibly because of solvation effects (Meyer et al., 1983; Shen et al., 1994). When the contributions of charged side chains are compared between similar 4Fe-4S redox proteins, the differences in the electrostatic interaction energies calculated from crystal structures do not correlate with the redox potential differences (Sweeney and Rabinowitz, 1980). Additionally, Warshel and co-workers have shown good correlation of electrostatic potential with experimental redox potentials in cytochrome *c* and 4Fe-4S proteins using a model in which the side chains that are normally charged at pH 7.0 are neutralized (Churg and Warshel, 1986; Langen et al., 1992a; Langen et al., 1992b). These results are compelling evidence that charged side chains at the surface contribute little to the redox potential. We therefore suggest that the observed differences in the redox potentials between homologous proteins can be explained by the differences in the contributions to the electrostatic potential of the backbone, polar side chains, and solvent.

In this paper, a series of calculations on four rubredoxins and four HiPIPs with known redox potentials and crystal structures are presented. Although our long term goal is to quantitatively predict the redox potentials of metalloproteins, the aim of this work was to identify structural deter

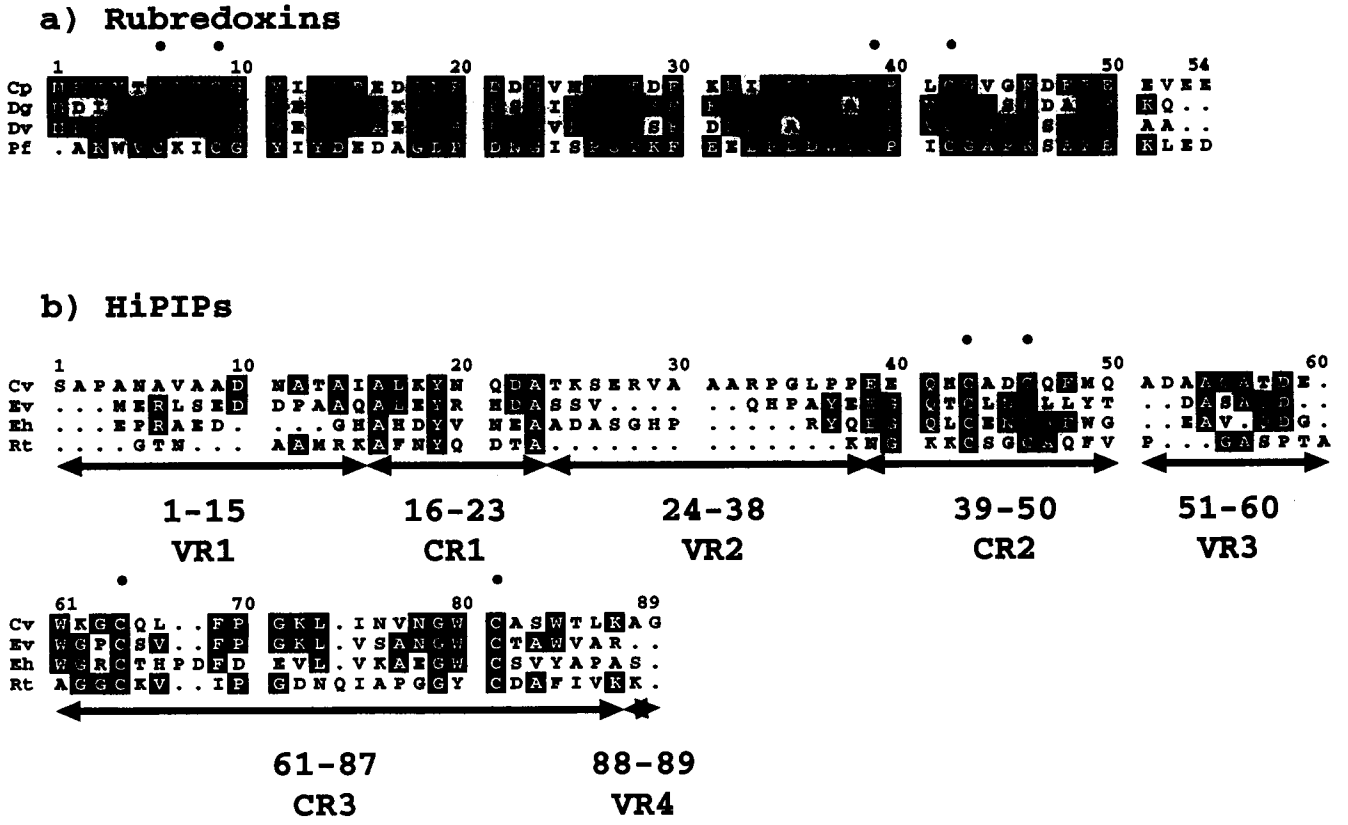

FIGURE 2 Sequence alignments for (*a*) rubredoxins and (*b*) high-potential iron sulfur proteins (HiPIPs) including core and variable region designations for HiPIPs. Cysteines are marked by black dots. These figures were generated using the program PRETTYBOX (Genetics Computer Group, 1994).

minants (i.e., specific residues) of the observed variations in the protein redox potentials. Thus, our methods were chosen based on the least coupling of the different components of the electrostatic potential. First, we analyzed crystal structures rather than structures resulting from energy minimizations or molecular dynamics simulations so that the structures themselves were independent of a given molecular mechanical potential energy parameter set. Second, we calculated the electrostatic potential at the center of the redox site, ϕ, by assuming that it is the sum of the Coulombic interactions of all of the partial charges, including that of the solvent (i.e., a dielectric continuum was not assumed, but rather an explicit molecular solvent was used). Therefore, the contribution of individual atoms to ϕ in our approach is simply additive and completely uncoupled from other atoms.

Based on the aforementioned experimental observations of the lack of importance of charged side chains at the surface, we focused on polar groups, although the contributions of charged side chains are not precluded by virtue of the additive approach. To further understand why charged side chains at the surface have so little effect on the redox potential in the rubredoxins, we first show the contribution of the charged side chains to ϕ to be largely dampened by solvent using an estimate of the solvation potential from molecular dynamics simulations. In the proteins that we studied, all of the charged side chains were farther than 9 Å from the redox site and were at the protein surface. Next, we addressed the question of whether the protein polar groups can explain the observed differences in redox potentials for rubredoxins and for HiPIPs. The ϕ due to protein polar groups for crystal structures of the four rubredoxins and the four HiPIPs were compared with experimentally measured redox potentials, and the differences in the contributions of specific sequence variants were identified. Although the aim was not so much to match the redox potentials, surprisingly good correlation was seen and, more importantly, structural differences giving rise to the redox potential variations were identified. Finally, suggestions for specific mutations to test these ideas are given.

METHODS

Three rubredoxin structures, from *Clostridium pasteurianum* (Cp) at 1.2-Å resolution (Watenpaugh et al., 1980), *Desulfovibrio gigas* (Dg) at 1.4-Å resolution (Frey et al., 1987), and *Desulfovibrio vulgaris* (Dv) at 1.5 Å (Adman et al., 1991), and the *Chromatium vinosum* (Cv) HiPIP structure at 2.0 Å (Carter et al., 1974) were obtained from the Brookhaven Protein Data Bank. The rubredoxin structure from *Pyrococcus furiosus* (Pf) at 1.8 Å was provided by Dr. Douglas Rees (Day et al., 1992). HiPIPs structures from *Ectothiorhodospira halophila* (Eh) at 1.5 Å, *Rhodocyclus tenuis* (Rt) at 1.5 Å, and *Ectothiorhodospira vacuolata* (Ev) at 1.8 Å were provided by Dr. Hazel Holden (Breiter et al., 1991; Rayment et al., 1992; Benning et al., 1994). All of the coordinates have since been deposited in the Brookhaven Protein Data Bank. Hydrogen positions were generated and energy-minimized with fixed bond lengths, resulting in only small changes between the

original generated positions and energy minimized positions (0.07 Å) and the electrostatic potentials (0.1 to 0.5 kcal/mol/e), using the molecular mechanics program CHARMM 22g3 and 24a3 (Brooks et al., 1983) .

The relationship between the standard free energy change upon reduction, ΔG, and the redox potential, $\mathscr{E}°$, is given by

$$-nF\Delta\mathscr{E}° = \Delta G = \Delta E - T\Delta S$$

where F is Faraday's constant, n is the number of electrons transferred, ΔE is the change in energy, T is the absolute temperature, and ΔS is the change in entropy. The change in energy due to the redox reaction may be divided into energy changes due to the charge change, $-n\phi$, where ϕ is the electrostatic potential at the redox center and that due to the relaxation of the protein and solvent. In this work, we examine $-n\phi$ and will examine the relaxation energy in detail elsewhere (Swartz and Ichiye, manuscript in preparation). This separation is addressed further in the Discussion section.

The electrostatic potential, ϕ, is given by

$$\phi = \sum_{i \neq \text{redox site}} \frac{Z_i}{r_i} \tag{1}$$

where Z_i is the charge of the ith atom, r_i is the distance from the ith atom to the redox center, and the sum is over all atoms i excluding the Fe, S, C, and H of the redox site. Because the sum extends over both protein and solvent, the dielectric is a constant throughout the system. Thus, the simple sum above is appropriate and effects due to dielectric screening, excluding electronic polarization, are included by the solvent contribution. If, instead, a protein is considered a low dielectric body immersed in a high dielectric media representing water, the potential must be solved for using the Poisson-Boltzmann equation (Gilson and Honig, 1988) and is no longer additive. Thus, ϕ can be broken down by limiting the sum to different types of atoms, i.e., backbone and side-chain polar groups, charged side-chain groups, and water. In the CHARMM potential, a group of atoms is defined as a set of adjacent atoms with a net integer charge, but with individual atoms of the group having partial charges (Brooks et al., 1983). Here, all electrostatic interactions are evaluated between the groups rather than the individual partially charged atoms because the electrostatics of a polar group with a net charge of zero is of much shorter range than the electrostatics of the individual partial charges comprising the group. The partial charges for Eq. 1 were obtained from the CHARMM 19 parameter set. Unfortunately, there are no good ways of assigning error to specific distances obtained from a crystal structure. However, a crude estimate was made of σ, the relative error in ϕ, using

$$\sigma = \left(\sum_i \frac{z_i^2}{r_i^4} \right)^{1/2} \Delta r \tag{2}$$

where Δr is the error in atomic position derived from the Luzzati plot (Luzzati, 1952) using the resolution and the R factor from the respective crystal structures.

Equation 1 also implies that the ϕ due to the solvent must be calculated. The solvation potential due to the nearby water, ϕ_{water}, is estimated by using molecular dynamics simulations of water around the fixed crystal structures of the proteins. The simulations were carried out at a system temperature of 300 K using CHARMM, as previously described (Yelle et al., 1995). The parameters used were those of CHARMM 19 for the protein (Brooks et al., 1983), TIP3P for water (Jorgensen, 1981), and additional parameters for the Fe-S site (Yelle et al., 1995). In this case, however, the protein coordinates were fixed in all calculations, all solvent molecules farther than 25 Å from a point 3 Å from the iron were deleted, free boundary conditions were used, a time step of 0.002 ps was used, and data were collected for 15 ps after 10 ps of equilibration. Averaging the solvent contributions to ϕ (Eq. 1) over the 15-ps collection period gives ϕ_{water}. Only waters within 23 Å of the redox center were included in this part of the calculations. The contributions of bulk water were obtained by two different approximations. The simplest estimate of the contribution of bulk water farther than 23 Å from the redox center, ϕ_{bulk}, comes from the Born equation:

$$\phi_{bulk} = -\left(1 - \frac{1}{\epsilon}\right)\frac{Q}{R} \tag{3}$$

where R = 23 Å, ϵ is the dielectric constant of water, and Q is the total charge of the protein. Note that this equation is for a potential energy rather than for the usual Born free energy (Hyun et al., 1995); multiplying by a factor of 1/2 Q yields the standard expression for the Born free energy of solvation. This model assumes the entire charge of the protein is concentrated in the center; i.e., the limiting expression far from the protein. A higher order approximation, ϕ^*_{bulk}, can be made that takes into account the arbitrary charge distribution of the protein (Hyun et al., 1995; Liu and Ichiye, 1994; Swartz, 1996),

$$\phi^*_{bulk} = 4\pi\rho\mu \int_{r>25\text{Å}} \left(\frac{\int \cos\gamma \exp[-\beta V_{Q\mu}] d\cos\gamma}{\int \exp[-\beta V_{Q\mu}] d\cos\gamma} \right) dr \tag{4}$$

where ρ is the molecular density, μ is the dipole moment of water, r is the radial distance from the water dipole to the iron, and γ is the angle between the iron-water internuclear vector and the water dipole vector. The energy, $V_{Q\mu}$, is given by

$$V_{Q\mu}(\vec{r}, \gamma) = \sum_i^N \frac{Q_i \mu \cos\gamma_i}{\epsilon' r_i^2} \tag{5}$$

where the subscript i refers to the ith atom and ϵ' is the appropriate screening for a dipole in a cavity (ϵ' = 19) (Hyun et al., 1995). The sum is over N, the total number of charges in the protein including that of the redox site. Equation 4 is evaluated numerically until it converges to the Born approximation at $r \approx 200$ Å.

RESULTS

The potential at the redox-site center, namely the iron for the rubredoxins and the center of the 4Fe-4S cubane structure for the HiPIPs, was chosen for the ease of calculation, but other positions such as the sulfurs are also reasonable locations to use. Although the most relevant quantity is the total interaction energy between the redox site and the rest of the protein, it is dependent on the charge distribution of the redox site, which has been described by vastly different potential charges (Noodleman et al., 1985; Mouesca et al., 1994; Koerner and Ichiye, submitted for publication). However, our choice of defining ϕ at the redox-site center is independent of the electrostatic parameters for the redox site.

Charged side chains and solvent

The degree of dampening of the charged side-chain contribution by water alone was studied by calculating the electrostatic contributions of each using the crystal structure coordinates for the charged side chains and using simulation data for surrounding water molecules plus approximations for the bulk water (see Methods). This study was carried out only for rubredoxins because of their smaller size. The charged side-chain contributions to ϕ (Table 1) are large and negative, ranging from −7.30 to −12.10 V. The solvent within 23 Å of the redox site, ϕ_{water}, contributes ~3.50 V to

TABLE 1 Electrostatic potentials at iron in rubredoxins

Rubredoxins	*D. gigas*	*D. vulgaris*	*P. furiosus*	*C. pasteurianum*
ϕ(CSC)	−8.02	−7.51	−7.35	−12.10
ϕ_{water}	3.32	3.69	1.98	3.36
ϕ_{bulk}	4.38	3.83	4.93	7.12
ϕ^*_{bulk}	4.54	4.00	5.52	7.84
ϕ(CSC) + ϕ_{water} + ϕ_{bulk}	−0.31	0.01	−0.44	−1.62
ϕ(CSC) + ϕ_{water} + ϕ^*_{bulk}	−0.15	0.17	0.15	−0.90

(CSC) is the potential due to charged side chains; ϕ_{water} is the potential calculated from simulation for solvent within 23 Å of the redox site; ϕ_{bulk} is the potential due to solvent farther than 23 Å of the redox site calculated using the Born approximation (Eq. 3); and ϕ^*_{bulk} is the potential due to solvent farther than 23 Å from the redox site calculated using the higher order approximation (Eq. 4). All values are given in eV.

ϕ for all but Pf, which has a lower value because of its greater protein volume. The contribution of solvent farther than 23 Å from the redox site by the Born approximation, ϕ_{bulk} (Eq. 3), is 3.85 to 7.10 V, whereas the higher order approximation, ϕ^*_{bulk} (Eq. 4), is 4.00 to 7.85 V (Table 1). Thus, relative to ϕ_{bulk}, ϕ^*_{bulk} is consistently higher and less dependent on the total charge. Overall, there is a large degree of cancellation between the charged side-chain and solvent contributions in both approximations. However, the cancellation is not complete and leads to deviations in ϕ between the four rubredoxins that are far greater than those between the experimental redox potentials. This is addressed further in the Discussion section.

Polar contributions

Because the charged side-chain contributions appear to be largely dampened by the solvent, the polar contributions to ϕ were calculated (Table 2). The polar contributions arise from the protein backbone as well as from polar side chains. In the CHARMM 19 parameters, all neutral residues except Ala, Gly, Ile, Leu, Phe, Pro, and Val have some polar character because of nonzero partial charges. The backbone also consists of two types of polar groups, one containing the amide N, H and C, and the other containing the carbonyl C and O. One notable feature of the total polar contributions is that they are very large and positive, ~2.5 V for the rubredoxins and ~1.1 V for the HiPIPs. Moreover, all polar groups that make significant contributions to ϕ occur within 8 Å of the redox site in the rubredoxins and within 10 Å of the redox site in the HiPIPs. In both cases, no charged side chains occur within these distances. In addition, although there are fairly large discrepancies between the ϕ and the experimental redox potentials, it is apparent that the polar contribution alone can account for the lower redox potential of Cp relative to the other rubredoxins as well as the higher values of Cv and Rt relative to Ev and Eh in the HiPIPs. The contributions for the HiPIPs are further broken down into those arising from a relatively constant core region (CR) and those from variable regions (VR) consisting of loops with different lengths (Figs. 1 *b* and 2 *b*), which were defined by least-squares fits of the backbones. Because Cv and Rt have core polar contributions that are ~0.6 V higher than those of Ev and Eh, it appears that the higher values of Cv and Rt relative to Ev and Eh arise within the core.

Contributions of individual residues for rubredoxins

The major polar contributions of the different protein sequences to the observed differences in ϕ among the four homologous rubredoxins are described here. Energy values

TABLE 2 Electrostatic potentials at the redox site due to backbone and polar sidechain dipoles and experimental redox potentials

Rubredoxins	*D. gigas*	*D. vulgaris*	*P. furiosus*	*C. pasteurianum*
Total charge	−8	−7	−9	−13
Redox potential*	0.006 ± 0.010[¶]	0.000 ± 0.010[‖]	0.000 ± 0.015[#]	−0.057[§]
ϕ(dipole)**	0.06 ± 0.09	0.00 ± 0.09	0.12 ± 0.18	−0.20 ± 0.09
HiPIPs	***C. vinosum***	***R. tenuis***	***E. vacuolata***	***E. halophila***
Total charge	−3	+4	−7	−11
Redox potential*	0.360[##]	0.330[##]	0.150[##]	0.120[##]
ϕ(Core dipoles)**	0.54 ± 0.15	0.63 ± 0.16	0.08 ± 0.16	−0.04 ± 0.15
ϕ(All dipoles)**	0.54 ± 0.16	0.38 ± 0.16	0.00 ± 0.16	0.13 ± 0.16

[#]Adams, 1992; [§]Lovenberg and Sobel, 1965; [¶]Moura et al., 1979; [‖]LeGall et al., 1988
[##]Meyer et al., 1983
*Redox potentials for *C. pasteurianum* and all HiPIPs were not reported with relative errors.
**Rubredoxin values are shown relative to *D. vulgaris* [ϕ(Dipole) = 2.547 eV]. HiPIP values are shown relative to *E. vacuolata* [ϕ(All Dipoles) = 0.833 eV]. In each case, Dv and Ev have the lowest dipole contribution of their respective protein type. Relative errors were calculated using Eq. 2.
All values given in eV.

are given both in units of kcal/mol/e and in mV (0.023 kcal/mol/e = 1 mV), and relevant distances from the iron are given in parentheses with the atom used to mark the distance noted. Overall, the errors computed (Eq. 2) are $<\sim$0.4 kcal/mol/e (20 mV) unless otherwise noted. The sequence alignment used for this comparison is shown in Fig. 2 *a*.

The backbone contributions to ϕ per residue are very similar among the four rubredoxins, with the largest contributions and also the largest variations near the iron coordination sites (Fig. 3 *b*). The variations here are primarily due to the orientations of the polar groups with respect to the iron atom rather than their distances from the iron, and these variations are subject to large errors (Eq. 2). For instance, there is a significantly increased contribution in Pf compared to the other rubredoxins because the amide group of Cys 42 is more oriented toward the Fe compared to the other three rubredoxins, thus raising ϕ by $\sim$2 kcal/mol/e (90 mV). However, because this group is close to the redox center (N, 3.62 Å), the relative error is large (1.4 kcal/mol/e) and therefore its contribution may not be significant (see Discussion). In fact, elimination of this contribution brings ϕ for Pf into better agreement with the redox potentials (Table 2). On the other hand, there is a structural explanation for the reduction in the backbone contribution from residues 43 and 44 in Cp, which each have contributions of ~ -0.5 kcal/mol/e (-20 mV). In this case, the Val 44 side chain in Cp occupies more space than the Ala 44 side chain occupies in the other rubredoxins, thus shifting Val 44 (N, 5.3 Å) farther from the iron than Ala 44 (*N*, 4.9 Å) of the other rubredoxins (Fig. 4) and rotating the backbone carbonyl of Gly 43 (C, 4.9 Å), a conserved residue.

The polar side-chain contribution to ϕ per residue is given in Fig. 3 *a* (note that charged side chains have no contribution in this figure). The most notable difference in the polar side-chain contribution is that residue 5 is a Thr (Oγ, 7.8 Å) in Cp with a contribution of ~ -2 kcal/mol/e (-100 mV) and a Val in the other three proteins with no contribution. The other major differences involve changes of polar to charged or polar to another polar side chain. Residue 7 is a Thr (Oγ, 8.0 Å) in Dv, Dg, and Cp, which has a negative contribution, whereas it is a Lys in Pf, which would give a positive contribution. Moreover, the contribution in Dv and Dg is almost 2 kcal/mol/e more negative than in Cp, which is caused by a rotation in the position of the Oγ hydrogen closer to the iron in Cp. Residue 22 has a change in the sign of the contribution because in Dv and Pf there is an Asn (Cγ, 12.1 Å) with a contribution of 1.5 kcal/mol/e (70 mV) that is replaced in Dg by a Ser with a contribution of -0.5 kcal/mol/e (-20 mV) and in Cp by an Asp, which would also be expected to give a negative contribution. However, the latter is probably too distant to be significant.

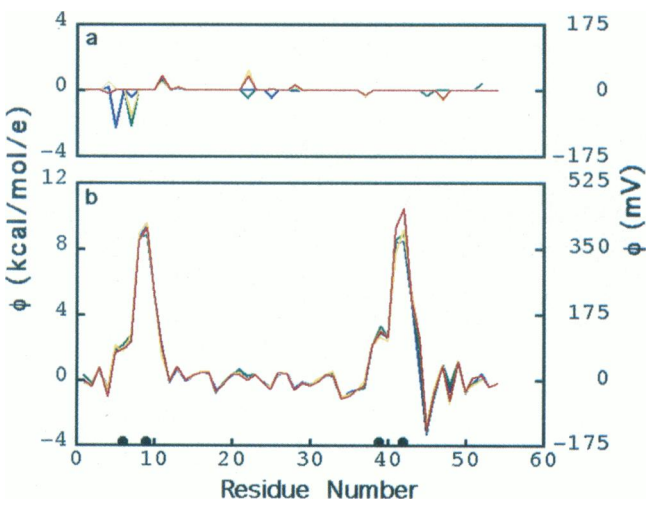

FIGURE 3 Electrostatic potential at the redox site per residue for *C. pasteurianum* (*blue*), *D. gigas* (*green*), *D. vulgaris* (*yellow*), and *P. furiosus* (*red*). (*a*) Polar side-chain contribution. (*b*) Backbone contribution. The residue numbers of cysteines which ligate the redox-site iron are indicated with black dots.

Contribution of individual residues for HiPIPs

The residues that have the major polar contributions in the four studied HiPIPs are described here. The largest variations in the polar contributions in the four variable regions are due primarily to insertions and deletions, especially in VR1 and VR2 (Figs. 1 *b* and 2 *b*). In VR1, the deletion of residues 10–13 in Eh raises the contribution of Eh by $\sim$5 kcal/mol/e (220 mV) relative to the other HiPIPs. The large 15 residue deletion in VR2 of Rt decreases the contribution to ϕ in Rt relative to the other HiPIPs by 3–4 kcal/mol/e (130–170 mV). In general, however, the total variable region polar contribution is $<\pm 6$ kcal/mol/e (260 mV), whereas the total core polar contribution is $\sim +26$ kcal/mol/e (1130 mV). Moreover, deletions in the protein are replaced by very polar solvent atoms, the analysis of which is beyond the scope of this study. As in the rubredoxins, the largest contributions are near the redox cluster coordination sites, which are in CR2 and CR3 (Figs. 1 *b*, 2 *b*, and 5 *b*).

The contributions of the core regions allow the four HiPIPs to be differentiated into two groups, as mentioned earlier. This differentiation can be seen in both the backbone and the polar side chains. For instance, the backbone carbonyls of residue 42 in Ev (O, 6.2 Å) and Eh (O, 6.4 Å) are shifted toward the redox site, relative to Cv and Rt (O, 6.6 Å), resulting in a nearly 1-kcal/mol/e (40 mV) decrease in their contribution to ϕ, although the source of the backbone shift is unclear. However, this residue is very close to the cubane, which has a radius of $\sim$4 Å, and as such has a large relative error (6 kcal/mol/e, 260 mV) and thus its contributions may not be significant. However, there are also several polar side chains in Ev and Eh that have more negative contributions to ϕ than in Cv and Rt. For instance, at position 45, Eh and Ev have an Asn (Cγ, 9.8 Å) that has a strong negative contribution to ϕ of -2 to -3 kcal/mol/e (-90 to -130 mV), whereas Cv and Rt have an Asp (which would also give a negative contribution) and Gly, respec

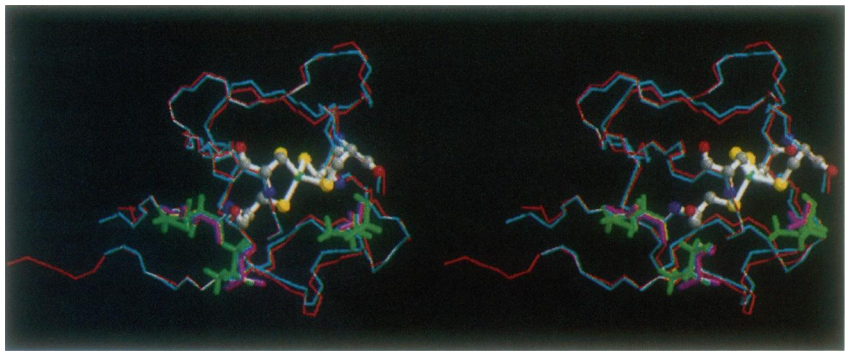

FIGURE 4 Stereo view of the backbone from *C. pasteurianum* (*red*) and *D. gigas* (*blue*) rubredoxins. A licorice-type rendering is used to illustrate residues 5, 7, and 44 showing the movement of the amide hydrogen of *C. pasteurianum* residue 44 farther from the iron (*green*) due to the larger size of the Val residue in *C. pasteurianum* relative to the Ala of *D. gigas* (*purple*). The rotation of the *C. pasteurianum* Thr 7 O_γ hydrogen farther from the iron is also shown. This figure was generated using MOLSCRIPT (Kraulis, 1991) and Raster3D (Merritt and Murphy, 1994).

tively, instead. This Asn 45 has the largest side-chain polar contribution seen in any of the HiPIPs because of its proximity to the redox site. In addition, two other large contributors to the negative character of Ev and Eh polar side chains occur at positions 65 and 82. In Eh, Thr 65 (Oγ, 8.5 Å) and Ser 82 (Oγ, 9.4 Å) each contribute −1.5 kcal/mol/e (−65 mV), whereas in Ev, Ser 65 and Thr 82 each contribute −1 kcal/mol/e (−50 mV). Cv has a Gln at position 65 that has a weak positive contribution of 0.5 kcal/mol/e (20 mV) and an Ala at position 82, whereas Rt has a Lys and Asp, respectively. Further, Rt not only has a Lys at residue 41, whereas the other three have a Gln (Cδ, 10.3 Å) that contributes −2 kcal/mol/e (70 mV), but also has a positive contribution of 1 kcal/mol/e (50 mV) from a Gln (Cδ, 7.0 Å) at residue 48, a position at which all other HiPIPs have nonpolar residues (Fig. 2 *b*). In addition, Cv has a strong, positive contribution of 3 kcal/mol/e (130 mV) from a Gln at residue 50 (Cδ, 10.3 Å), a position at which all other HiPIPs have contributions of only 1 kcal/mol/e (40 mV) or less. Overall, Ev and Eh appear to have similar lower redox potentials due to similarities in their core regions, whereas Cv and Rt appear to have higher redox potentials than Ev and Eh due to different residues.

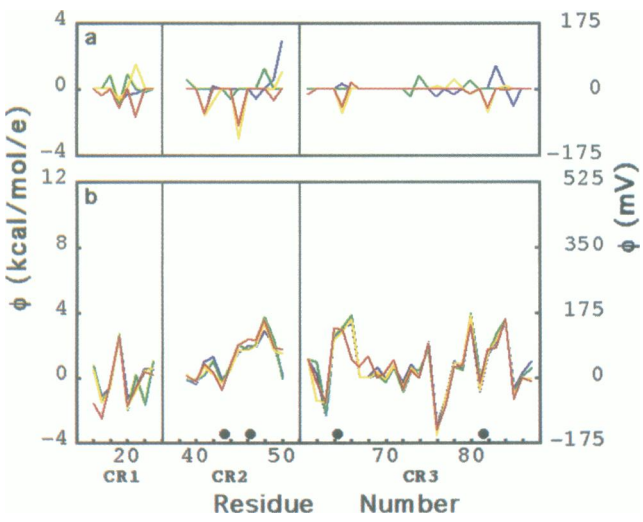

FIGURE 5 Contribution of core region polar groups to electrostatic potential for *C. vinosum* (*blue*), *R. tenuis* (*green*), *E. vacuolata* (*yellow*), and *E. halophila* (*red*). (*a*) Polar side-chain contribution. (*b*) Backbone contribution. Residue numbers of cysteines which ligate the redox site are indicated with black dots. Breaks in the sequences due to variable loop regions are indicated by vertical lines.

DISCUSSION

Calculations of ϕ for homologous Fe-S proteins were used here to understand the structural origins of redox potentials. There are two types of contributions to ϕ from the protein: charge interactions due to charged side chains and polar interactions from both the backbone and polar side chains. The largest protein contribution to ϕ comes from residues with charged side chains; however, there are many indications that this contribution is dampened by other factors, including solvation, as outlined in the Introduction. Our results for rubredoxin suggest that the contributions of

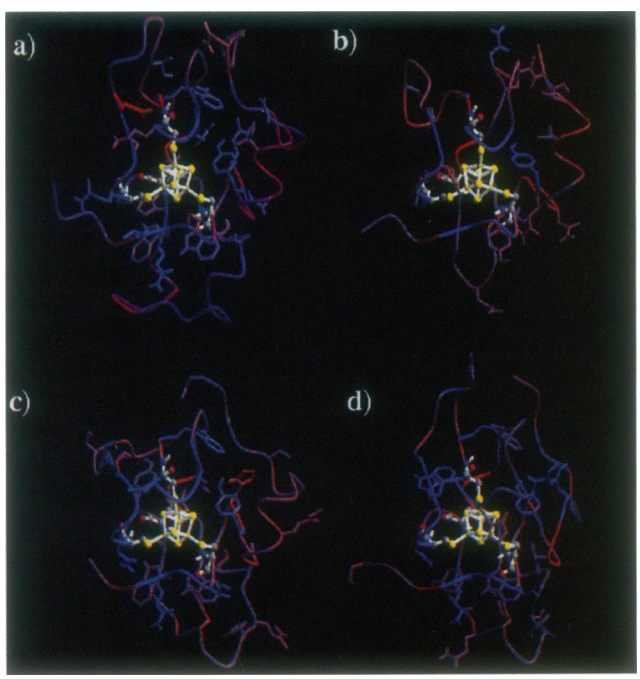

FIGURE 6 Contribution of backbone and polar side-chain groups to ϕ in the HiPIPs. Groups are smoothly colored from red (negative) to blue (positive) according to their contribution. (*a*) *C. vinosum* (*b*) *R. tenuis* (*c*) *E. vacuolata* (*d*) *E. halophila*. This figure was generated using MOLSCRIPT (Kraulis, 1991) and Raster3D (Merritt and Murphy, 1994).

charged residues to ϕ are largely reduced by water alone (Table 1), which is a molecular interpretation of the dielectric screening effects of water. In addition, other factors beyond the scope of these calculations such as the effect of counterions may further offset the charged side-chain contribution (Yelle et al., 1995). The other major protein contributions to ϕ are the polar groups. Generally, the contribution to ϕ of only the backbone and side-chain polar groups appears to correlate with the redox potential, although the magnitudes of the variations in ϕ are greater, for both the rubredoxins and the HiPIPs, a finding similar to that of Churg and Warshel (1986) and Langen et al. (1992b).

Despite the apparent agreement of the calculated ϕ from the polar protein groups with the experimental redox potentials, this type of calculation is a qualitative rather than quantitative prediction of redox potentials because of the approximations made. First, the energy due to protein relaxation upon reduction of the protein is neglected (Shenoy and Ichiye, 1993), because crystal structures for both oxidation states are available only for Pf rubredoxin (Day et al., 1992). On the other hand, energy minimization studies of homologous rubredoxins indicate that the relaxation energies bring ϕ into even better agreement with the redox potentials (Swartz and Ichiye, manuscript in preparation). Molecular dynamics simulations of Cp rubredoxin indicate an even more dramatic change upon reduction in that water penetrates near the redox site (Yelle et al., 1995), although this has yet to be confirmed experimentally. However, crystal structures are studied here because the structures have errors associated only with the x-ray experiment and not from inadequacies in a potential energy field, which structures from energy minimization and molecular dynamics would reflect. The only part of the CHARMM potential that is used in these calculations is the partial charges of the protein, excluding the redox site (and thus, this is also a test of the partial charges). More generally, entropic and dynamic effects are neglected by not using molecular dynamics, but these are likely to be small for the highly homologous rubredoxins.

Another approximation, which is related to protein relaxation, involves electronic polarization. This effect is treated implicitly via the partial charges in the CHARMM potential, which were optimized to give good protein structure. This approach has been highly successful for liquids (Jorgensen and Swenson, 1985; Jorgensen, 1981), and more recent studies of ionic solutions with polarizable water models indicate that electronic polarization is unimportant unless the charge of the ion is >2 (D. Smith, personal communication). However, the most effective use of implicit electronic polarization is when nuclear relaxation (i.e., protein relaxation) is included.

A final reason that the calculation does not quantitatively predict redox potentials is the approximate treatment of the solvent and charged side-chain contributions. The molecular dynamics simulations of water around the frozen crystal structure of the protein neglect the dynamics of the protein and counterions. However, both the similar size and structure of the rubredoxins and the lack of correlation of the size of the HiPIPs with the redox potentials indicate that the differences in redox potential are not controlled by differences in the solvent accessibility. Furthermore, the calculations of the solvent dampening cannot be interpreted as a complete cancellation of charged side-chain contributions, but rather as a means of understanding why mutations involving charged side chains at the surface have so little effect on observed redox potentials (Shen et al., 1994; Gleason, 1992; Zeng et al., 1996; Schejter and Eaton, 1984). In fact, the pH dependence of the redox potentials of redox proteins, for instance, Pf Rd (Adams, 1992) indicates that ionizable groups may play a role, which could possibly be because of local unfolding or protonation of the redox site or, more simply, because of the electrostatic effect of changing the net charge of the protein. However, given that experiments have shown that mutations of charged side chains at the surface generally have little effect, these calculations show that those few with significant contributions will be hard to identify because they will involve the balance between several large effects. Thus, these calculations further support the idea that polar groups are worth examining as structural determinants of the overall protein redox potential and that they are better candidates for mutation as their contributions are easier to quantify.

Our approximations can be compared with those in other calculations of redox potentials of Fe-S proteins, such as those on HiPIPs and ferredoxins (Langen et al., 1992b; Jensen et al., 1994). Warshel and co-workers generally use their protein dipole Langevin dipole method, which, unlike the methods here, includes electronic polarization explicitly. In addition, the surrounding aqueous environment is treated as a cubic grid of Langevin dipoles and charged side chains are neutralized. The protein dipole Langevin dipole method has not been completely successful in predicting redox potential trends in the ferredoxins (Jensen et al., 1994); however, their overall body of work, including studies of cytochrome *c* (Churg and Warshel, 1986; Langen et al., 1992a) and the photosynthetic reaction center (Parson et al., 1990), seems to indicate the lack of importance of charged side chains. Our results, using very different potential functions actually support the latter conclusion at least for surface residues. However, perhaps the greatest difference between this paper and the works of Warshel et al. is that our focus is on determining specific structural determinants as opposed to predicting redox potentials. Moreover, the additivity of ϕ in our calculations makes it straightforward to assess the contribution of individual residues and it is thus complementary to the Poisson-Boltzmann approach used in programs like DelPhi (Gilson and Honig, 1988), which would give a better assessment of the total electrostatic potential including dielectrically screened charged side chains, although the decomposition of individual contributions is more difficult.

Despite the fact that the calculations are only qualitative for the prediction of redox potentials, several important

conclusions can be made. First, the large overall positive contribution indicates that the polar groups are highly oriented around the redox site with the positive ends of the dipoles pointing toward the site, thus stabilizing the net negative charge on the redox site. Although the contribution appears larger in rubredoxins than in HiPIPs, the larger radius of the redox site in the HiPIPs means that the nearest protein atom is further from the redox-site center and thus the contribution is attenuated. In addition, structural reasons for the observed differences in redox potentials among the homologous rubredoxins and among the homologous HiPIPs have been identified.

In the rubredoxins, the structural differences that cause Cp to have a lower redox potential than Dg, Dv, and Pf are reflected in ϕ. This is apparently due to a backbone shift caused by the presence of Val at residue 44 in Cp rather than an Ala as in the other three rubredoxins. Furthermore, of nine homologous single Fe rubredoxins with sequence and redox potentials (Table 4), the four (including Cp) with redox potentials from -61 to -40 mV all have Val at position 44, and the five (including Pf, Dv, and Dg) with redox potentials from 0 to $\sim$42 mV all have Ala at position 44. The *Heliobacillus mobilis* rubredoxin is particularly striking because it has the least negative charge of all nine but has a redox potential of -46 mV, whereas the others with redox potentials near -50 mV tend to have more negative charges than the ones with redox potentials near 0 mV. Interestingly, the contribution of residue 44 is the "incipient" hydrogen bond noted by Adman et al. (1975). Moreover, the poorer results for Pf are likely to be due to the large error in the backbone contribution of residue 42. The side chain of Thr 5 in Cp may also play a role in its lower redox potential, although this is not reflected in the sequence data and it is much more distant than the backbone of residue 44.

Among the HiPIPs, Ev and Eh are lower in redox potential than Cv and Rt, which is also reflected in the ϕ. In fact, this trend is seen in the ϕ due to the core alone, which explains why Cv and Rt are alike in their redox potentials, whereas they are the most different in size (85 vs. 62 residues) of the four HiPIPs studied. This is useful to know because not only are the loop positions subject to packing forces in the crystal structures but they may fluctuate in solution as well. Moreover, it is difficult to predict the position of engineered loops. The low redox potential of Ev and Eh is largely due to the presence of polar side chains with negative contributions to ϕ at residues 45, 65, and 82 in Eh and Ev. In addition, the backbone at residue 42 may play a role in altering the redox potential, but the source of the backbone shift has not been identified and the error in the potentials at this close distance is large. It is also interesting to note that the conserved NH···S bonds noted in Backes et al. (1991) give similar contributions and thus do not contribute to differences within this homologous set, in agreement with their analysis. Thus, the lower redox potential of Ev and Eh appears to be due to the more negative contributions of the polar side chains (and possibly the backbone) of several residues.

Experimental measurement of the effect of site specific mutations on redox potentials is a means of verifying our results. As the residues that contribute most to ϕ among the two groups of proteins were identified in the previous section, certain mutations are suggested based on the following rationale. Predictions based on mutations to or from residues with solvent exposed charged side chains are avoided because the effects of such mutations have previously been shown to either not significantly affect redox potentials if they are close to the redox site (Shen et al., 1994; Gleason, 1992; Schejter and Eaton, 1984) or to alter them unpredictably (Zeng et al., 1996). The best choices are therefore mutations of residues with polar side chains not involved in intramolecular hydrogen bonding, because it is difficult to predict the exact position of a mutated side chain with a nonpolar side chain that is of similar size. In general, large polar contributions very near to or very far from the redox site were considered suspect. Close to the redox site, the differences between homologous proteins were in the contributions of like backbone groups rather than the substitution of a polar for nonpolar side chain. However, at close distances, a slight error in the position or orientation will lead to large changes in ϕ. Therefore, unless some structural explanation could be found supporting the shift in the polar group position or orientation, these variations were viewed as less promising (though still possible) candidates for mutagenesis. On the other hand, polar contributions very far from the redox site, generally the substitution of a polar

TABLE 3 Proposed mutations in rubredoxins and HiPIPs along with their contribution to the electrostatic potential at the redox site and the proposed direction of the resultant change in redox potential

Protein	Mutation	Contribution to ϕ (mV)	Redox potential
Rubredoxin			
Cp	Val44Ala	-40*	Increase
Cp	Thr5Val	-100	Increase
Dg#, Dv#	Thr7Val	-90	Increase
Dv, Pf, Dg	Ala44Val	$+40$*	Decrease
Dv§	Asn22Leu	$+70$	Decrease
Pf§	Asn22Leu	$+70$	Decrease
HiPIP			
Eh#, Ev#	Asn45Leu	-90 to -130	Increase
Eh, Ev#, Cv#	Gln41Leu	-70	Increase
Eh	Thr65Val	-50	Increase
Ev	Ser65Ala	-65	Increase
Eh	Ser82Ala	-50	Increase
Ev	Thr82Val	-65	Increase
Rt	Gln48Leu	$+50$	Decrease
Cv	Gln50Leu	$+130$	Decrease

*Total contribution of residues 43 and 44. See Results.

#Involved in intramolecular hydrogen bond. Here, an intramolecular hydrogen bond is defined to have a donor-acceptor distance of less than 4 Å, a donor-hydrogen-acceptor angle within 45° of linearity, and a hydrogen-acceptor-antecedent angle within 80° of linearity.

§Probably too distant ($\sim$12 Å).

TABLE 4 Amino acid sequence alignments, redox potentials ($\mathscr{E}°$), and net peptide charges of single [Fe] rubredoxins (adapted from Zeng et al., 1995)

Rubredoxin*	Amino acid sequence#						$\mathscr{E}°$ (mV), NHE	Net charge§
	1	10	20	30	40	50		
Cl	MQKYVCSVCG	YVYDPADGEP	DDPIDPGTGF	EDLPEDWVCP	VCGVDKDLFE	PES	−61	−12.0
Cp	MKKYTCTVCG	YIYNPEDGDP	DNGVNPGTDF	KDIPDDWVCP	LCGVGKDQFE	EVEE	−57	−9.0
Hm¶	MKKYGCLVCG	YVYDPAKGDP	DHGIAPGTAF	EDLPADWVCP	LCGVSKDEFE	PL	−46	−5.0
Bm	MQKYVCDICG	YVYDPAVGDP	DNGVAPGTAF	ADLPEDWVCP	ECGVSKDEFS	PEA	−40	−9.0
Pf	AKWVCKICG	YIYDEDAGDP	DNGISPGTKF	EELPDDWVCP	ICGAPKSEFE	KLED	0	−8.0
Dv	MKKYVCTVCG	YEYDPAEGDP	DNGVKPGTSF	DDLPADWVCP	VCGAPKSEFE	AA	0	−6.0
Dv (M)	MKKYVCTVCG	YEYDPAEGDP	DNGVKPGTAF	EDVPADWVCP	ICGAPKSEFE	PA	+5	−6.0
Dg	MDIYVCTVCG	YEYDPAKGDP	DSGIKPGTKF	EDLPDDWACP	VCGASKDAFE	KQ	+6	−6.0
Me	MDKYECSICG	YIYDEAEGD•	DGNVAAGTKF	ADLPADWVCP	TCGADKDAFV	KMD	+23, +42	−8.0
	• •				•	• ⇑		

Cl, *Chlorobium limicola* f. sp. thiosulfatophilum; Cp, *Clostridium pasteurianum*; Hm, *Heliobacillus mobilis*; Bm, *Butyribacterium methylotrophicum*; Pf, *Pyrococcus furiosis*; Dv, *Desulfovibrio vulgaris*, strain Hildenborough; Dv(M), *Desulfovibrio vulgaris*, strain Miyazaki; Dg, *Desulfovibrio gigas*; Me, *Megasphaera elsedenii*.

#The numbering system for *Clostridium pasteurianum* rubredoxin is used throughout.

§Net charge of the apoprotein calculated at neutral pH (−1 for D, E, C-terminus; +1 for K, R, N-terminus).

¶(Lee et al., 1995)

•, Cysteine ligands to the Fe; ⇑, position of Ala/Val 44.

for nonpolar side chain, are more likely to be screened dielectrically. Finally, it must be noted that because only energetic contributions from the existing native crystal structures have been calculated and because mutations may cause perturbations of the protein structure, the magnitude of the changes in redox potential induced by the mutations cannot be predicted from these calculations.

Candidates for site specific mutagenesis in the rubredoxins are given in Table 3 along with their contribution to ϕ and whether they are involved in intramolecular hydrogen bonds. The best candidate for the source of the 60-mV lower redox potential of Cp relative to the other three rubredoxins is the occurrence of Val, rather than Ala, at residue 44, as this substitution alters the backbone contribution. We therefore suggest the mutation of Val 44 to Ala in Cp or Ala 44 to Val in Dv, Dg, or Pf as a test of the importance of this difference. Another possibility is the occurrence of Thr 5 in Cp rather than Val, as in the other rubredoxins. Mutation of Thr 5 to Val should result in an increase in the redox potential of Cp. Such a mutation also allows one to determine if the much more distant polar side chain at residue 5 has as much influence on the redox potential as the backbone at residue 44. Similarly, the other mutations listed in Table 3 would also indicate whether these side chains are too distant to have appreciable effects on the redox potential.

Candidates for mutations of the HiPIPs are also given in Table 3. Although insertion and deletion mutants of variable loop regions are possible candidates, predicting the effects of such mutations on the redox potential is beyond the scope of this study, because the loops are likely to be both flexible and cause differential solvation of the protein. Moreover, because the core regions have much stronger polar side-chain contributions than do the variable regions, only point mutations for the core region will be suggested. Testing the structural origins of the lower redox potentials of Ev and Eh is more difficult because they appear to be due to the generally more negative character of several residues. Further, the structural cause of the backbone shift at residue 42 is not clear and residues 45, 65, and 82 are more distant. The mutations proposed for residues 45, 65, and 82 are the best candidates for increasing the redox potentials of Ev and Eh. In addition, other mutations would also affect the redox potentials, such as replacement of Gln 41 in Eh, Ev, or Cv with a nonpolar residue, resulting in a relative increase, or replacement of Gln 48 in Rt and Gln 50 in Cv, resulting in a relative decrease.

CONCLUSIONS

The results presented here demonstrate that, of the various contributions to the electrostatic potential at the redox site, the charged side chain contribution is largely cancelled by solvent effects in the rubredoxins, and the backbone and polar side-chain contributions together can explain the differences in the experimental redox potentials between the homologous rubredoxins and between homologous HiPIPs. For both rubredoxins and HiPIPs, the backbone contribution is large and positive, indicating that it is polarized around the redox site. In addition, the residues in the rubredoxins and the HiPIPs that are responsible for the major variations in ϕ have been identified. In the rubredoxins, the results show that the backbone shift due to the presence of Val, rather than Ala, at residue 44 in Cp is a likely source of its lower redox potential relative to the other three rubredoxins. The presence of Thr 5 in Cp rather than Val as in the other three rubredoxins is also a possible cause, however, this is not substantiated by other sequence data. Interestingly, in the HiPIPs, the contribution of the core polar groups appears to be responsible for the separation in redox potentials between the two HiPIPs with higher values (Cv and Rt), and

the two with lower values (Ev and Eh), explaining why the two HiPIPs with the greatest size difference, namely Cv and Rt, have similar redox potentials. The lower redox potentials of Ev and Eh, relative to Cv and Rt, appear to be due to a more negative environment created by several residues in Ev and Eh as opposed to one or two key residues.

The authors would like to thank Drs. Douglas Rees and Hazel Holden for providing coordinates and special thanks to Dr. Hazel Holden for providing coordinates for *E. vacuolata* before publication. We also thank the Visualization, Analysis and Design in the Molecular Sciences Laboratory at Washington State University and the Maui High Performance Computing Center for computational resources.

This work was supported by grant GM45303 from the National Institutes of Health and grants MCB-9118985, MCB-9506796 from the National Science Foundation. Research performed at the Maui High Performance Computing Center is sponsored in part by the Phillips Laboratory, Air Force Materiel Command, USAF, under cooperative agreement number F29601-93-2-0001.

The views and conclusions contained in this document are those of the authors and should not be interpreted as necessarily representing the official policies or endorsements, either expressed or implied, of Phillips Laboratory or the U.S. Government.

REFERENCES

Adams, M. 1992. Novel iron-sulfur centers in metalloenzymes and redox proteins from extremely thermophilic bacteria. *Adv. Inorg. Chem.* 38: 341–396.

Adman, E., L. C. Sieker, and L. Jensen. 1991. Structure of rubredoxin from *Desulfovibrio vulgaris* at 1.5 Å resolution. *J. Mol. Biol.* 217:337–352.

Adman, E., K. D. Watenpaugh, and L. H. Jensen. 1975. The H-S hydrogen bonds in *Peptococcus aerogenes* ferredoxin, *Clostridium pasteurianum* rubredoxin and *Chromatium vinosum* high potential iron protein. *Proc. Natl. Acad. Sci. USA.* 72:4854–4858.

Armstrong, F. 1982. Oxidation-reduction and substitution reactions of iron-sulphur centers. *In* Advances in Inorganic and Bioinorganic Mechanisms. Academic Press, London. 65–120.

Backes, G., Y. Mino, T. M. Loehr, T. E. Meyer, M. A. Cusanovich, W. V. Sweeney, E. T. Adman, and J. Sanders-Loehr. 1991. The environment of the Fe_4S_4 clusters in ferredoxins and high-potential iron proteins. New information from x-ray crystallography and resonance Raman spectroscopy. *J. Am. Chem. Soc.* 113:2055–2064.

Benning, M. M., T. E. Meyer, I. Rayment, and H. M. Holden. 1994. Molecular structure of the oxidized high-potential iron-sulfur protein isolated from *Ectothiorhodospira vacuolata. Biochemistry.* 33: 2476–2483.

Breiter, D. R., T. E. Meyer, I. Rayment, and H. Holden. 1991. The molecular structure of the high potential iron-sulfur protein isolated from *Ectothiorhodospira halophila* determined at 2.5 Å resolution. *J. Biol. Chem.* 226:18660–18667.

Brooks, B., R. E. Bruccoleri, B. D. Olafson, D. J. States, S. Swaminathan, and M. Karplus. 1983. CHARMM: A program for macromolecular energy, minimization, and dynamics calculations. *J. Comp. Chem.* 4:187–217.

Cammack, R. 1992. Iron-sulfur cluster in enzymes: themes and variations. *In* Iron-Sulfur Proteins. Academic Press, Inc., San Diego. 281–322.

Carter, C. W., J. Kraut, S. T. Freer, N.-H. Xuong, R. A. Alden, and R. G. Bartsch. 1974. Two-angstrom crystal structure of oxidized *Chromatium* high potential iron protein. *J. Biol. Chem.* 249:4212–4225.

Churg, A. K., and A. Warshel. 1986. Control of the redox potential of cytochrome *c* and microscopic dielectric effects in proteins. *Biochemistry.* 25:1675–1681.

Day, M. W., B. T. Hsu, L. Joshua-Tor, J.-B. Park, Z. H. Zhou, M. W. W. Adams, and D. C. Rees. 1992. X-ray crystal structures of the oxidized and reduced forms of the rubredoxin from the marine hyperthermophilic archebacterium *Pyrococcus furiosus. Protein Sci.* 1:1494–1507.

Frey, M. W., L. Sieker, F. Payan, R. Haser, M. Bruschi, G. Pepe, and J. LeGall. 1987. Rubredoxin from *Desulfovibrio gigas*. A molecular model of the oxidized form at 1.4 Å resolution. *J. Mol. Biol.* 197:525–541.

Genetics Computer Group. 1994. Program Manual for the Wisconsin Package, 575 Science Drive, Madison, Wisconsin, USA 53711.

Gilson, M. K., and B. H. Honig. 1988. Calculation of the total electrostatic energy of a macromolecular system: solution energies, binding energies, and conformational analysis. *Proteins.* 4:7–18.

Gleason, F. K. 1992. Mutation of conserved residues in *Escherichia coli* thioredoxin: effects on stability and function. *Protein Sci.* 1:609–616.

Gunner, M. R., and B. Honig. 1991. Electrostatic control of midpoint potentials in the cytochrome subunit of the *Rhodopseudomonas viridis* reaction center. *Proc. Natl. Acad. Sci. USA.* 88:9151–9155.

Hyun, J. K., C. S. Babu, and T. Ichiye. 1995. Apparent local dielectric response around ions in water: a method for its determination and its applications. *J. Phys. Chem.* 99:5187–5195.

Jensen, G. M., A. Warshel, and P. J. Stephens. 1994. Calculation of the redox potentials of iron-sulfur proteins: the 2-/3- couple of $[Fe_4S^*4Cys_4]$ clusters in *Peptococcus Aerogenes* ferredoxin, *Azotobacter vinelandii* ferredoxin I, and *Chromatium vinosum* high-potential iron protein. *Biochemistry.* 33:10911–10924.

Jorgensen, W. L. 1981. Transferable intermolecular potential functions for water, alcohols, and ethers. Application to liquid water. *J. Am. Chem. Soc.* 103:335–340.

Jorgensen, W. L., and C. J. Swenson. 1985. Optimized intermolecular potential functions for amides and peptides. Structure and properties of liquids amides. *J. Am. Chem. Soc.* 107:569–578.

Kraulis, P. J. 1991. MOLSCRIPT: a program to produce both detailed and schematic plots of protein structures. *J. Appl. Cryst.* 24:946–950.

Langen, R., G. D. Brayer, A. M. Berghuis, G. McLendon, F. Sherman, and A. Warshel. 1992a. Effect of the Asn52-Ile mutation on the redox potential of yeast cytochrome *c*. Theory and experiment. *J. Mol. Biol.* 224:589–600.

Langen, R., G. M. Jensen, U. Jacob, P. J. Stephens, and A. Warshel. 1992b. Protein control of iron-sulfur cluster redox potentials. *J. Biol. Chem.* 267:25625–25627.

Lee, W. Y., D. C. Brune, R. LoBrutto, and R. E. Blankenship. 1995. Isolation, characterization, and primary structure of rubredoxin from the photosynthetic bacterium, *Heliobacillus mobilis. Arch. Biochem. Biophys.* 318:80–88.

LeGall, J., B. C. Prickril, I. Moura, A. V. Xavier, J. J. Moura, and B. H. Huynh. 1988. Isolation and characterization of rubrerythrin, a non-heme iron protein from *Desulfovibrio vulgaris* that contains rubredoxin centers and a hemerythrin-binuclear iron cluster. *Biochemistry.* 27:1636–1642.

Liu, Y., and T. Ichiye. 1994. An integral equation theory for the structure of water around globular solutes. *Chem. Phys. Lett.* 231:380–386.

Lovenberg, W., and B. Sobel. 1965. Rubredoxin: a new electron transfer protein from *Clostridium pasteurianum. Proc. Natl. Acad. Sci. USA.* 54:193–199.

Luzzati, V. 1952. Traitement 'stastique des erreurs dans la determination des structures cristallines. *Acta Cryst.* 5:802–810.

Matsubara, H., and K. Saeki. 1992. Structural and functional diversity of ferredoxins and related proteins. *In* Iron-Sulfur Proteins. Academic Press, Inc., San Diego. 223–281.

Merritt, E. A., and M. E. P. Murphy. 1994. Raster3D Version 2.0: a program for photorealistic molecular graphics. *Acta Cryst.* D50: 869–873.

Meyer, T. E., J. A. Prezysiecki, J. A. Watkins, A. Bhattacharyya, R. P. Simondsen, M. A. Cusanovich, and G. Tollin. 1983. Correlation between rate constant for reduction and redox potential as a basis for systematic investigation of reaction mechanisms of electron transfer proteins. *Proc. Natl. Acad. Sci. U.S.A.* 80:6740–6744.

Mouesca, J. M., J. L. Chen, L. Noodleman, D. Bashford, and D. A. Case. 1994. Density functional/Poisson-Boltzmann calculations of redox potentials for iron-sulfur clusters. *J. Am. Chem. Soc.* 116:11898–11914.

Moura, I., J. J. G. Moura, M. H. Santos, A. V. Xavier, and J. LeGall. 1979. Redox studies on rubredoxin from sulphate and sulphur reducing bacteria. *FEBS Lett.* 107:419–421.

Noodleman, L., J. G. Norman, J. H. Osborne, A. Aizman, and D. A. Case. 1985. Models for ferredoxins: electronic structures of iron-sulfur clusters with one, two, and four iron atoms. *J. Am. Chem. Soc.* 107:3418–3426.

Parson, W. W., Z.-T. Chu, and A. Warshel. 1990. Electrostatic control of charge separation in bacterial photosynthesis. *Biochim. Biophys. Acta.* 1017:251–272.

Rayment, I., G. Wesenberg, T. E. Meyer, M. A. Cusanovich, and H. M. Holden. 1992. Three-dimensional structure of the high-potential iron-sulfur protein isolated from purple phototropic bacterium *Rhodocyclus tenuis* determined and refined at 1.5 Å resolution. *J. Mol. Biol.* 228: 672–686.

Schejter, A., and W. A. Eaton. 1984. Charge-transfer optical spectra, electron paramagnetic resonance, and redox potentials of cytochromes. *Biochemistry.* 23:1081–1084.

Shen, B., D. R. Jollie, C. D. Stout, T. C. Diller, F. A. Armstrong, C. M. Gorst, G. N. La Mar, P. J. Stephens, and B. K. Burgess. 1994. *Azotobacter vinelandii* ferredoxin I: alteration of individual surface charges and the $[4Fe\text{-}4S]^{2+/+}$ cluster reduction potential. *J. Biol. Chem.* 269: 8564–8575.

Shenoy, V. S., and T. Ichiye. 1993. Influence of protein flexibility on the redox potential of rubredoxin: energy minimization studies. *Proteins.* 17:152–160.

Sieker, L. C., R. E. Stenkamp, L. H. Jensen, B. Pickril, and J. LeGall. 1986. Structure of rubredoxin from the bacterium *Desulfovibrio desulfuricans. FEBS Lett.* 208:73–76.

Swartz, P. D. 1996. Computational models of redox proteins and protein model building. Ph. D Thesis. Washington State University.

Sweeney, W. V., and J. C. Rabinowitz. 1980. Proteins containing 4Fe-4S clusters: an overview. *Ann. Rev. Biochem.* 49:139–161.

Watenpaugh, K. D., L. C. Sieker, and L. H. Jensen. 1980. Crystallographic refinement of rubredoxin at 1.2 Å resolution. *J. Mol. Biol.* 138:615–633.

Yelle, R. B., N. S. Park, and T. Ichiye. 1995. Molecular dynamics simulations of rubredoxin from *Clostridium pasteurianum*: changes in structure and electrostatic potential during redox reactions. *Proteins Struct. Funct. Genet.* 22:154–167.

Zeng, Q., E. T. Smith, D. M. Kurtz, and R. A. Scott. 1996. Protein determinants of metal site reduction potentials: site directed mutagenesis studies of *Clostridium pasteurianum* rubredoxin. *Inorg. Chim. Acta.* 242:245–251.